ACS APPLIED MATERIALS & INTERFACES

Research Article

www.acsami.org

Bipyrene-Functionalized Graphene as a "Turn-On" Fluorescence Sensor for Manganese(II) Ions in Living cells

Xiaowei Mao,[†] Haiyan Su,[†] Demei Tian,[†] Haibing Li,*[,†] and Ronghua Yang[‡]

[†]Key Laboratory of Pesticide & Chemical Biology (CCNU), Ministry of Education; College of Chemistry, Central China Normal University, Wuhan 430079, P.R. China

[‡]State Key Laboratory of Chem/Biosensing and Chemometrics, College of Chemistry and Chemical Engineering, Hunan University, Changsha, 410082, P.R. China

Supporting Information

ABSTRACT: 1,2-bis-(2-pyren-1-ylmethylamino-ethoxy) ethane (NPEY) was synthesized and brought to the surface of graphene nanosheets (GNs) via $\pi-\pi$ stacking, which provided a simple and convenient route for processing "turn-on" fluorescent sensor by simply mixing the diluted aqueous solutions of both components. The synthesized NPEY modified graphene nanosheets (NPEY-GNs) not only allows good selectivity toward Mn^{2+} with the detection limit of 4.6×10^{-5} M, but also shows "turn-on" response for Mn^{2+} both in vitro and in living cells. These sensing capabilities of NPEY-GNs in living cells make it a robust candidate for many biological fields, such as intracellular tracking, intracellular imaging, etc.

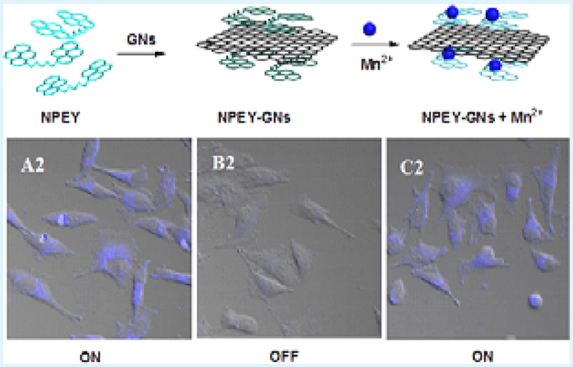

KEYWORDS: *graphene, fluorescence, turn on, sensor, electron transfer, manganese(II) ions*

1. INTRODUCTION

Designing and synthesizing highly sensitive and selective chemosensors for heavy metal ions have become increasingly important because of their close relationship with environmental and human health.[1,2] To date, numerous reports have been made for the detection of different metal ions, such as Hg^{2+},[3] Pb^{2+},[4,5] Ni^{2+},[6,7] Cd^{2+},[8−10] etc. However, novel chemosensors are required to achieve the goal of extensively recognizing other heavy metal ions. Mn^{2+}, as a typical heavy metal ion, is an essential trace metal closely related to human health. Extracellular Mn^{2+} inhibits Ca^{2+} influx through cell membranes and therefore inhibits contractions of smooth muscle, which is not conducive to the growth of bone.[11−13] More importantly, Mn^{2+} not only serves as a cofactor for enzymes such as decarboxylase, hydolase, and kinase but also is involved in the metabolism of protein, lipid, and carbohydrate.[14] Recently, a number of Mn^{2+} fluorescent sensors have been reported because of their simplicity and unparalleled sensitivity. Canary and co-workers employed fluorescent "turn-on" probes for Mn^{2+} and Ca^{2+} determination in living cells based on a soft ligand.[15] Cui and his co-workers further demonstrated that a pH-controlled recognition method for the discriminative detection of Mn^{2+} and Cu^{2+} via QD fluorescence quenching sensing.[16] Nevertheless, the aforementioned Mn^{2+} fluorescent probes suffer multiple shortcomings, including lack of selectivity, or fluorescence quenching, and these are significant problems in practical application. Therefore, there is an urgent need to develop new fluorescence "turn-on" receptors with high selectivity for Mn^{2+} detection.

Graphene nanosheets (GNs), emerged as a new class of carbon materials that only one atom thick, have attracted increasing interest because of its excellent dimensional mechanical, structural, and electrical properties.[17−19] Owing to its unique characteristics, GNs receptors have been broadly studied and used in quantum electrical devices,[20,21] nanocomposites,[22] electromechanical resonators,[23] and gas or pH sensors.[24,25] GNs also exhibits a fascinating property for fluorescence-quenching capability by electron or energy transfer, and the extraordinarily wonderful property allows this new materials to be potentially used in fluorescent detection.[26,27] For instance, the fluorescent "turn-on" graphene sensor, based on dye-labeled aptamer assemble on graphene system, was employed as sensing devices for the detection of important biomolecules,[28−30] metal ions[31−33] and bimolecular events,[34−43] etc. Although progresses have been achieved, the detection in most graphene sensor relies on the use of dye-labeled aptamer or single-stranded DNA, which is expensive and prone to denaturation. Thus alternative, developing new and improved GNs-based sensor simultaneously processing high efficiency and "turn on" fluorescent signal is highly desirable.

Received: September 10, 2012
Accepted: January 17, 2013
Published: January 17, 2013

Pyrene and its derivatives, acted as a widely used fluorescent output group for fluorescent probe design, had been reported previously for their noncovalent interactions with graphene via π-stacking.[44−50] Herein, we report a simple and convenient route to produce novel NPEY-GNs as "turn-on" fluorescence sensor for Mn^{2+} recognition. In our strategy, pyrene derivative 1, 2-bis-(2-pyren-1-ylmethylamino-ethoxy) ethane (NPEY),[51] utilized as ideal fluorescent reporting groups for heavy metal ions probe design, was used to embellish graphene surface via $\pi-\pi$ stacking for producing the NPEY-GNs receptor (Scheme 1). The potential application of NPEY-GNs as a "turn on" fluorescence sensor for Mn^{2+} both in vitro and in living cells was also investigated.

Scheme 1. Synthetic Route for NPEY-GNs

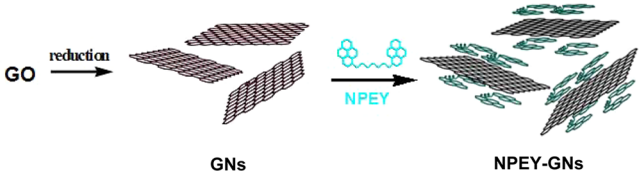

2. EXPERIMENTAL SECTION

2.1. Materials. All chemicals and solvents unless otherwise specified were analytical grade, and distilled water were used throughout. Graphite, hydrazine solution (≥85 wt %), and ammonia solution (25−28 wt %) was purchased from sinopharm chemical reagent Beijing Co., Ltd. (SCRC, China). All anion samples were obtained from Shanghai chemical factory, China. All anion samples were chloride salts and prepared with aqueous solution.

2.2. Apparatus. The UV source was a 250 W high-pressure fluorescent Hg lamp with the strongest emission at 365 nm (Institute of Electrical Light Source, Beijing). Fluorescence spectra were taken on a FluoroMax-P luminescence spectrometer (Horiba Jobin Yvon Inc.). The infrared (IR) spectra were collected on a spectrometer (Thermo Nicolet Nexus IR) in the wavenumber range 400−4000 cm^{-1} at a resolution of 4 cm^{-1}. The high resolution transmission electron microscopy (HRTEM) image of GNs was measured by a TEM (JEM-2100F). Tapping mode atomic force microscopy (AFM) characterizations were conducted on a Nanoscope III (Digital Instrument) scanning probe microscope. Confocal images were acquired using a Zeiss confocal laser scanning unit mounted on a LSM710 fixed-stage upright microscope. Images were recorded using 40×/0.75 M27 oil-immersion objective. The laser excitation for NPEY-GNs is 390 nm, and the fluorescence detection band was set to 438−502 nm. The ultrasonic bath was a SB120D supersonic instrument.

2.3. Preparation of NPEY-Modified Graphene Sheet. Graphene oxide was obtained by method developed by Hummers and Offemann.[52,53] Considering the stronger $\pi-\pi$ stacking interactions between NPEY and GNs,[44] GO was reduced to obtain GNs in this work. The as-made homogeneous yellow solution of single layer GO was reduced by hydrazine to remove the oxygenous groups according to the procedures reported by Li and co-workers.[54] After the reduction, a black dispersion with a small amount of black precipitate was obtained. Successively, this dispersion was filtered through glass cotton to remove the precipitate and yield a stable black aqueous dispersion of GNs. Afterward, 0.5 mL of NPEY (10^{-3} M THF solution) was injected into 20 mL GNs (0.05 mg/mL) solution for the preparing of NPEY-GNs, as shown in Scheme 1, and then the as-synthesized sample was treated by centrifugalization method and washed by water for 3 times to remove the excess of NPEY. Finally, the obtained product was further characterized by IR, AFM, and TEM.

2.4. Cell Culture and Fluorescence Microscopy. Hela cells were grown in dulbecco's modified eagles medium (DMEM, Invitrogen, USA) supplemented with 10% fetal calf serum (FBS). The cells were seeded in tissue culture plates and incubated in a fully humidified atmosphere at 37 °C containing 5% CO_2.[55] Hela cells were grown on glass coverslips placed at the bottom of 24-well culture plates. In this experiment, the medium was replaced with fresh medium containing the materials NPEY (1×10^{-3} M). After 2 h of treatment, the coverslips were removed, washed three times with phosphate-buffered saline (PBS), and then fluorescence images were taken with a confocal fluorescence microscope (Figure 4A, A1, and A2). Hela cells incubated with NPEY for 2 h, being washed with cold PBS, and then incubated with fresh medium containing GNs at a concentration of 0.25 mg/mL for 2 h. Afterward, the aforementioned cell dish was rinsed with PBS then observed under a confocal fluorescence microscope (Figure 4B, B1, and B2). Being treated with NPEY and GNs as described above, cells were further incubated in medium containing Mn^{2+} (1×10^{-3} M), fluorescence images were taken after being washed with cold PBS (Figure 4C, C1, and C2).

3. RESULTS AND DISCUSSION

The NPEY-GNs maintain benign water solubility for more than 1 week, and it was characterized by UV−vis spectroscopy, AFM, TEM, FT-IR, and fluorescence studies. Above all, the formation of single-layer GNs through exfoliation and the morphological information on NPEY-GNs was revealed by AFM measurement. As shown in Figure 1A, the thickness of

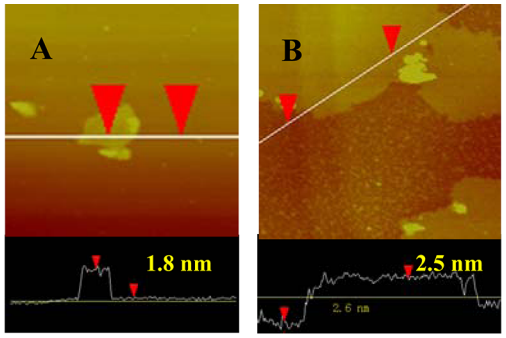

Figure 1. AFM images of (A) GNs, (B) NPEY-GNs.

GNs is 1.8 nm, which is a typically thickness of single-layer graphene according to previous work,[17−43] whereas the height of NPEY-GNs displayed by AFM was increased to 2.5 nm (Figure 1B). It is reported that the distance between 1-pyrenebutyrate and graphene sheet through $\pi-\pi$ stackings is 0.35 nm according to previous literature.[56,57] Comparing with the thickness of GNs and NPEY-GNs demonstrates that monolayered NPEY molecules covered both sides of GNs with offset face-to-face orientation via $\pi-\pi$ interactions. Additionally, Figure S1 in the Supporting Information shows the HRTEM image of NPEY-GNs, evidencing the successful NPEY decorations endowed GNs accordingly. Furthermore, the interaction between GNs and NPEY was fully investigated by means of UV−vis. Figure S2 in the Supporting Information shows UV−vis spectra of NPEY, GNs and NPEY-GNs. The absorption peaks of free NPEY to bound NPEY-GNs are slightly broadened and red-shifted: the two characteristic peaks of NPEY shifts from 289, 340 to 297 ($\Delta\lambda$ = 8 nm), 348 ($\Delta\lambda$ = 8 nm), respectively. Similarly, the absorption peak of GNs from 262 to 268 nm ($\Delta\lambda$ = 6 nm). This is indicative of $\pi-\pi$ interactions between NPEY and GNs.[58] In addition, FT-IR was carried out to further characterize the noncovalent functionalization process of NPEY molecules on GNs. As shown in Figure S3 in the Supporting Information, it is clear from FT-IR

dx.doi.org/10.1021/am3026807 | ACS Appl. Mater. Interfaces 2013, 5, 592−597

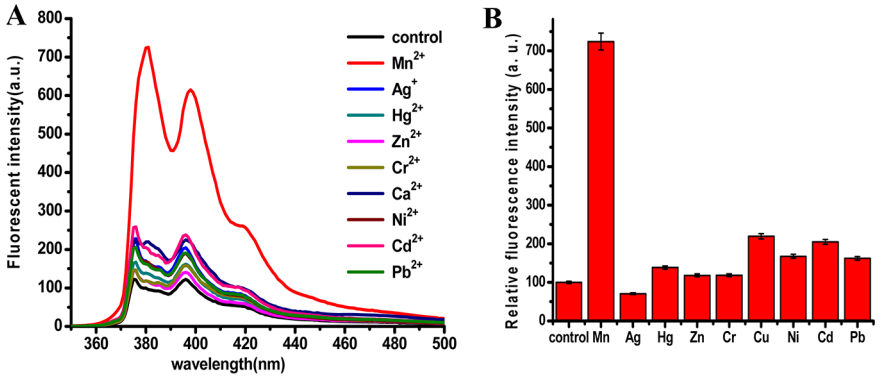

Figure 2. (A) Fluorescence emission responses of NPEY-GNs system to different metal ions. (B) The hisgram directly shows the changes of fluorescence emission of NPEY-GNs at 376 nm with adding of different heavy metal ions, respectively.

Scheme 2. (Center) Schematic Demonstration of Fluorescence "Turn-On" Mechanism for Mn^{2+} Detection by NPEY-GNs; Fluorescence Emission Changes of (Left) NPEY-GNs and (Right) NPEY-GNs in the Presence of Mn^{2+} under Illumination by UV Light at 365 nm

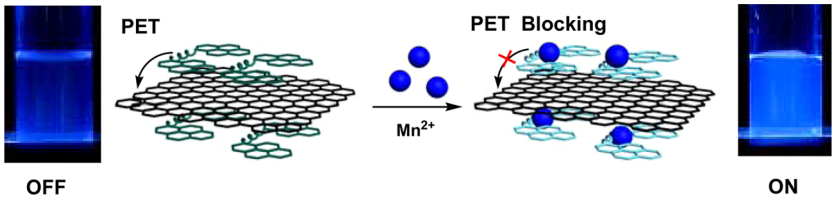

spectrum of NPEY that the typical absorption features of the C−H stretching vibrations at 2900 cm^{-1} and N−H stretching vibrations at 3039 cm^{-1}. When compared with the FT-IR spectrum of NPEY-GNs, with C−H stretching vibrations at 2900 cm^{-1} and N−H stretching vibrations at 3039 cm^{-1} still kept intact, this clearly confirms that NPEY molecules are successfully embellish the surface of GNs. Moreover, further evidence for the noncovalent decoration comes from photoluminescence measurements. In the fluorescence spectra (see Figure S4 in the Supporting Information), characteristic emission band of NPEY at 376 and 396 nm is ascribed to its excimer emission, whereas this emission was greatly quenched by GNs, indicating that a photoinduced electron transfer (PET) process was taken place between NPEY molecules and GNs via $\pi-\pi$ stacking interactions.[59,60]

Having successfully functionalized NPEY with GNs, we further demonstrated the potential application of NPEY-GNs as fluorescence sensor toward fluorescence measurement. In order to confirm the selectivity of NPEY-GNs probe, representative heavy metal ions (Mn^{2+}, Ag^{+}, Cd^{2+}, Cr^{2+}, Ca^{2+}, Hg^{2+}, Ni^{2+}, Pb^{2+}, and Zn^{2+}) of the same concentration (0.1 mL, 1×10^{-3} M) were added to the solution of NPEY-GNs (3 mL). As depicted in Figure 2, the spectrum of the free NPEY-GNs showed two weak emission bands at 376 and 396 nm, which could be the result of fluorescence quenching through the PET process. Only Mn^{2+} induced a dramatic increase in the fluorescence intensity of NPEY-GNs, accompanying an obviously bright blue emission under illumination by UV light at 365 nm (inset image in Figure 2). To rule out the possibility of the fluorescence recovery induced by free NPEY binding with Mn^{2+} in the solution, a control experiment was done in which the NPEY solution mixed with Mn^{2+} solution (see Figure S4 in the Supporting Information). Although NPEY exhibited an emission peak at 376 and 396 nm, its intensity was remained unchanged even after the addition of Mn^{2+} under the same conditions, suggesting that fluorescence recovery is not electron transfer between NPEY and Mn^{2+}. Furthermore, GNs upon adding Mn^{2+} was characterized by AFM to check the interaction between GNs and Mn^{2+}. Seen from the AFM images in Figure S5 in the Supporting Information, the thickness of GNs is 1.8 nm with no obviously folding and aggregation, indicating the GNs alone can not serve as a senor for Mn^{2+}. The results depicted above showed that NPEY-GNs exhibited a high selectivity in sensing Mn^{2+} toward other heavy metal ions accompanying with a phenomenon of fluorescent "on". A schematic of the fluorescent "on" process is shown in Scheme 2. It is reported that multiethylene-glycol groups can provide binding sites to transition metal ions.[61−63] In the meantime, imino groups can improve the binding of metal ions. Mn^{2+}, classified as "hard" metal, can form stronger complexes with oxygen donors and appears to be more tolerant of softer atom donors than other metal ions.[64] As a result, the multiethylene-glycol groups and imino groups from NPEY are inclined to coupling with Mn^{2+} (see Figure S6 in the Supporting Information). Because of the bind of Mn^{2+} to the NPEY at oxygen donor and imino groups, the electron transfer between NPEY and GNs was disrupted due to "blocking" effect, leading to a significantly enhanced fluorescence emission. To validate the expanded application of the NPEY-GNs platform, the anti-interference experiments are conducted in the presence of a mixture of various representative interference ions (0.1 mL, 5×10^{-3} M Co^{+}, Cr^{2+}, Cd^{2+}, Cu^{2+}, Ag^{+}, Pb^{2+}, Zn^{2+}, and Hg^{2+}), with the subsequent addition of Mn^{2+} (0.1 mL, 10^{-3} M). As shown in Figure S7 in the Supporting Information, no significant fluorescent recovery except for Mn^{2+}, indicating this NPEY-GNs sensor is highly selective with negligible interference. As described above, we can reasonably deduce that electron transfer process take place when NPEY molecule first attached to GNs, and then the electron transfer

dx.doi.org/10.1021/am3026807 | ACS Appl. Mater. Interfaces 2013, 5, 592−597

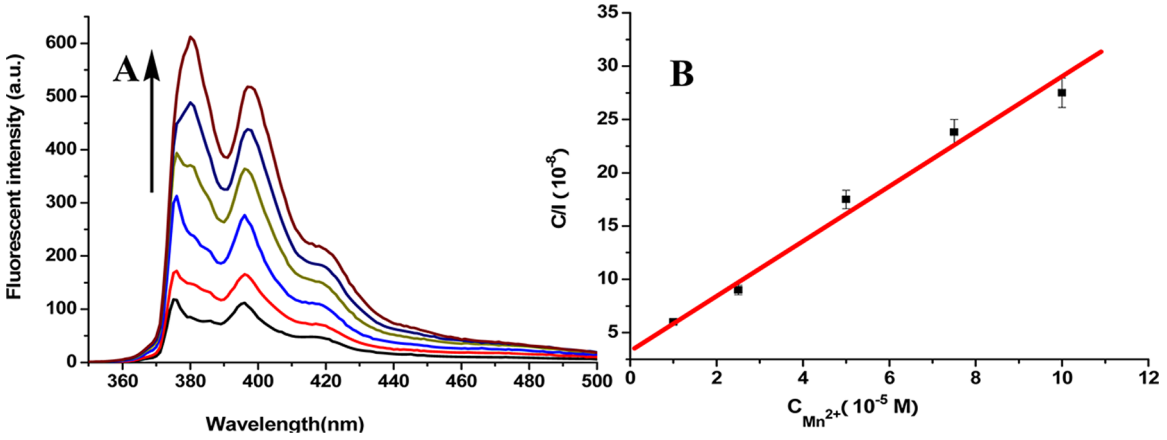

Figure 3. (A) Fluorescence spectra of NEPY-GNs in the presence of different concentrations of Mn^{2+}: 0.1, 0.25, 0.5, 0.75, 1, 2.5, and 5 μM. (B) Mn^{2+} concentration-dependent fluorescence intensity plot with a fitting curve based on a Langmuir binding model (376 nm).

process was blocked by the addition of Mn^{2+} accompanying with fluorescence "off and on".

To gain insight into the recognition ability of NPEY-GNs, we added a series of different Mn^{2+} concentration ranging from 1×10^{-5} M to 10×10^{-5} M to the NPEY-GNs solution. Figure 3A shows the effect of increasing concentration of Mn^{2+} on the fluorescence emission intensity of NPEY-GNs. It is clear that with the concentration of Mn^{2+} increased, the fluorescence emission intensity of NPEY-GNs was progressively enhanced, which also suggest a blocked PET signaling mechanisms of the NPEY to GNs by Mn^{2+}. The growth of fluorescence with increasing concentration of the Mn^{2+} was well fitted by a Langmuir-type binding model. A good linear relationship was found on dependence of C/I as a function of C (C is the concentration of Mn^{2+}, and I is the fluorescence intensity of NPEY-GNs at given Mn^{2+} concentrations) is shown in Figure. 3B. On the basis of the 3σ IUPAC criteria, the detection of Mn^{2+} concentration based on the synthesized NPEY-GNs sensor is 4.6×10^{-5} M.

After exploring the sensing property of NPEY-GNs in vitro, we further analyzed its recognition ability for Mn^{2+} in living cells. For this purpose, Hela cells incubated with NPEY in growth media up to 2 h at 37 °C exhibited a blue-green color throughout the whole cells (Figure 4A2), suggesting that NPEY were taken up by HeLa cells. A significantly fluorescence decreases could be observed for Hela cells incubated with GNs (Figure 4B2) after complete washing and rinsing with PBS, indicating successful intracellular GNs delivery in living cells. According to the pervious studies,[65−69] graphene-based materials could be efficiently transported into living cells, and the uptake of graphene-based materials possibly relies on direct penetration of cell membranes. Therefore, it is reasonable to believe that both the cellular uptake of GNs and the electron transfer from NPEY to GNs process was taken place in cells from observing fluorescence quenching of Hela cells. Afterward, Hela cells incubated with Mn^{2+}, which had been treated with NPEY-GNs for 4 h, were observed by confocal microscopy. The fluorescence images showed conspicuous blue emission accompanying the entrance of Mn^{2+} into the cells, as can be seen from Figure 4C2, suggesting a blocked electron transfer signaling mechanisms upon adding Mn^{2+} was taken place in the cells. On the basis of the results described above, we can draw a conclusion that the designed NPEY-GNs probe can be used to image intracellular Mn^{2+} in living cells by using a general fluorescence technique, which should be potentially useful for the study of intracellular imaging and intracellular tracking, etc.

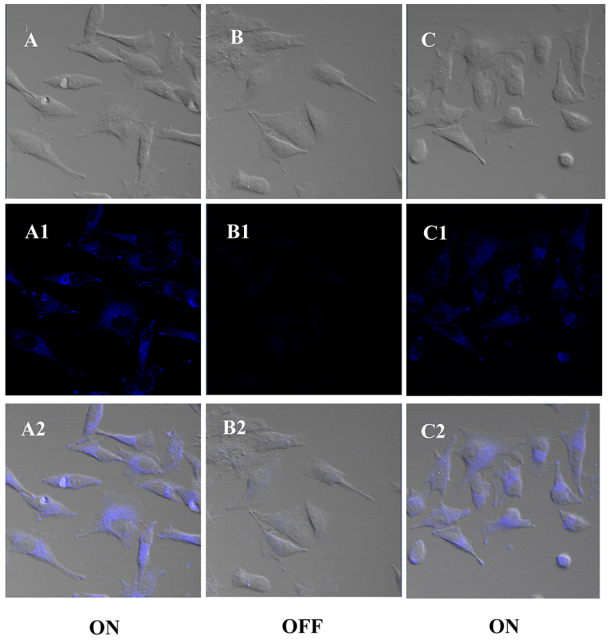

Figure 4. Confocal fluorescence microscopy images of Hela cells were incubated with NPEY(A, A1, A2) without GNs or (B, B1, B2) with GNs; and (C, C1, C2) with NPEY, GNs, Mn^{2+} in sequence for 2−4 h at 37 °C. Images were obtained after extensive washing of cells with PBS. Bright-field (top), dark-field fluorescence (middle), and overlap of images of dark and bright field (bottom), respectively.

4. CONCLUSIONS

In summary, we illustrated a simple and convenient methodology for synthesizing a novel NPEY-GNs fluorescence sensor with excellent selectivity for Mn^{2+} through a PET signaling mechanism. Significantly, imaging and detecting Mn^{2+} in living cells has also been accomplished. We believe this novel probes may expand the application of graphene-based materials to other fields, including intracellular tracking, intracellular imaging, living cells monitoring, etc.

dx.doi.org/10.1021/am3026807 | ACS Appl. Mater. Interfaces 2013, 5, 592−597

■ ASSOCIATED CONTENT

Supporting Information

^{1}HNMR and ^{13}CNMR spectra of Compound NPEY; UV/vis absorption, FT-IR spectra and fluorescence spectra of GNs, NPEY-GNs, and NPEY, respectively; the fluorescence spectra of anti-interference experiments in the presence of a mixture of various representative interference ions. This material is available free of charge via the Internet at http://pubs.acs.org.

■ AUTHOR INFORMATION

Corresponding Author

*Tel.: +86-27-67866423. E-mail: lhbing@mail.ccnu.edu.cn.

Notes

The authors declare the following competing financial interest(s): This work was financially supported by the National Natural Science Foundation of China (21072072, 21102051), PCSIRT (NO.IRTO953), Program for New Century Excellent Talent in University (NCET-10-0428), Self-determined research funds of CCNU from the colleges basic research and operation of MOE (CCNU11C01002, CCNU12A01004, CCNU12A02012), and State Key Laboratory of Chemo/Biosensing and Chemometrics (201003).

■ ACKNOWLEDGMENTS

This work was financially supported by the National Natural Science Foundation of China (21072072, 21102051), PCSIRT (IRTO953), Program for New Century Excellent Talent in University (NCET-10-0428), Self-determined research funds of CCNU from the colleges' basic research and operation of MOE (CCNU11C01002, CCNU12A01004, CCNU12A02012), and State Key Laboratory of Chemo/Biosensing and Chemometrics (201003).

■ REFERENCES

(1) Hao, H.; Wang, G.; Sun, J. *Drug Metab. Rev.* **2005**, *37*, 215−234.
(2) Brown, J. M.; Davies, S. G. *Nature* **1989**, *342*, 631−636.
(3) Ou, J. J.; Kong, L.; Pan, C. S.; Su, X. Y.; Lei, X. Y.; Zou, H. F. *J. Chromatogr. A* **2006**, *1117*, 163−169.
(4) Sun, P.; Krishnan, A.; Yadav, A.; Singh, S.; MacDonnell, F. M.; Armstrong, D. W. *Inorg. Chem.* **2007**, *46*, 10312−10320.
(5) Slama, I.; Dufresne, C.; Jourdan, E.; Fahrat, F.; Villet, A.; Ravel, A.; Grosset, C.; Peyrin, E. *Anal. Chem.* **2002**, *74*, 520−526.
(6) Lammers, I.; Buijs, J.; Ariese, F.; Gooijer, C. *Anal. Chem.* **2009**, *81*, 6226−6233.
(7) Lammers, I.; Buijs, J.; Ariese, F.; Gooijer, C. *Anal. Chem.* **2010**, *82*, 9410−9417.
(8) Pu, L. *Chem. Rev.* **2004**, *104*, 1687−1716.
(9) McCarroll, M. E.; Billiot, F. H.; Warner, I. M. *J. Am. Chem. Soc.* **2001**, *123*, 3173−3174.
(10) Han, C. P.; Li, H. B. *Small* **2008**, *4*, 1344−1350.
(11) Khotari, H. M.; Kulp, E. A.; Nakanishi, S.; Switzer, J. A. *Chem. Mater.* **2004**, *16*, 4232−4244.
(12) Doménech, A.; Alarcón, J. *Anal. Chem.* **2007**, *79*, 6742−6751.
(13) Limmer, S. J.; Kulp, E. A.; Switzer, J. A. *Langmuir* **2006**, *22*, 10535−10539.
(14) Takeda, A. *Brain Research Reviews* **2003**, *41*, 79−87.
(15) Liang, J.; Canary, J. W. *Angew. Chem., Int. Ed.* **2010**, *49*, 7710−7713.
(16) Xu, S. H.; Wang, C. L.; Cui, Y. P. *J. Mater. Chem.* **2012**, *22*, 9216−9221.
(17) Allen, M. J.; Tung, V. C.; Kaner, R. B. *Chem. Rev.* **2010**, *110*, 132−145.
(18) Rao, C. N. R.; Sood, A. K.; Govindaraj, A. *Angew. Chem., Int, Ed.* **2009**, *48*, 7752−7777.
(19) Geim, A. K. *Science* **2009**, *324*, 1530−1534.
(20) Xia, J.; Chen, F.; Li, J. H.; Tao, N. *Nat. Nanotechnol.* **2009**, *4*, 505−509.
(21) Chen, F.; Qing, Q.; Xia, J.; Li, J. H.; Tao, N. *J. Am. Chem. Soc.* **2009**, *131*, 9908−9909.
(22) Stankovich, S.; Dikin, D. A.; Dommett, G. H. B.; Kohlhaas, K. M.; Zimney, E. J.; Stach, E. A.; Piner, R. D.; Nguyen, S. T.; Ruoff, R. S. *Nature* **2006**, *442*, 282−286.
(23) Bunch, J. S.; Zande, A. M.; Verbridge, S. S.; Frank, I. W.; Tanenbaum, D. M.; Parpia, J. M.; Craighead, H. G.; McEuen, P. L. *Science* **2007**, *315*, 490−493.
(24) Robinson, J. T.; Perkins, F. K.; Snow, E. S.; Wei, Z.; Sheehan, P. E. *Nano Lett.* **2008**, *8*, 3137−3140.
(25) Ang, P. K.; Chen, W.; Wee, A. T. S.; Loh, K. P. *J. Am. Chem. Soc.* **2008**, *130*, 14392−14393.
(26) Swathi, R. S.; Sebastiana, K. L. *J. Chem. Phys.* **2008**, *129*, 054703.
(27) Swathi, R. S.; Sebastiana, K. L. *J. Chem. Phys.* **2009**, *130*, 086101.
(28) Jang, H.; Kim, Y. K.; Kwon, H. M.; Yeo, W. S.; Kim, D. E.; Min, D. H. *Angew. Chem., Int. Ed.* **2010**, *49*, 5703−5707.
(29) Wang, X.; Wang, C.; Qu, K.; Song, Y.; Ren, J.; Miyoshi, D.; Sugimoto, N.; Qu, X. *Adv. Funct. Mater.* **2010**, *20*, 3967−3971.
(30) Li, J. J.; Lu, C. H.; Yao, Q. H.; Zhang, X. L.; Liu, J. J.; Yang, H. H.; Chen, G. N. *Biosens. Bioelectron.* **2011**, *26*, 3894−3899.
(31) Wen, Y.; Xing, F.; He, S.; Song, S.; Wang, L.; Long, Y.; Li, D.; Fan, C. *Chem. Commun.* **2010**, *46*, 2596−2598.
(32) Wu, W.; Hu, H.; Li, F.; Wang, L.; Gao, J.; Lu, J.; Fan, C. *Chem. Commun.* **2011**, *47*, 1201−1203.
(33) Shi, Y.; Huang, W. T.; Luo, H. Q.; Li, N. B. *Chem. Commun.* **2011**, *47*, 4676−4678.
(34) Chang, H.; Tang, L.; Wang, Y.; Jiang, J.; Li, J. *Anal. Chem.* **2010**, *82*, 2341−2346.
(35) Li, F.; Huang, Y.; Yang, Q.; Zhong, Z.; Li, D.; Wang, L.; Song, S.; Fan, C. *Nanoscale* **2010**, *2*, 1021−1026.
(36) Mao, X. W.; Tian, D. M.; Li, H. B. *Chem. Commun.* **2012**, *48*, 4851−4853.
(37) Wen, Y.; Peng, C.; Li, D.; Zhuo, L.; He, S.; Wang, L.; Huang, Q.; Xu, Q. H.; Fan, C. *Chem. Commun.* **2011**, *47*, 6278−6280.
(38) Sheng, L.; Ren, J.; Miao, Y.; Wang, J.; Wang, E. *Biosens. Bioelectron.* **2011**, *26*, 3494−3499.
(39)
(40) Lu, C. H.; Li, J.; Lin, M. H.; Wang, Y.; Yang, W.; Chen, H. H.; Chen, X. *Angew. Chem., Int. Ed.* **2010**, *49*, 8454−8457.
(41) Wang, Y.; Li, Z.; Hu, D.; Lin, C. T.; Li, J.; Lin, Y. *J. Am. Chem. Soc.* **2010**, *132*, 9274−9276.
(42) Wang, H.; Zhang, Q.; Chu, X.; Chen, T.; Ge, J.; Yu, R. *Angew. Chem., Int. Ed.* **2011**, *50*, 7065−7069.
(43) Bhunia, S. K.; Jana, N. R. *ACS Appl. Mater. Interfaces* **2011**, *3*, 3335−3341.
(44) Xu, Y. X.; Bai, H.; Lu, G. W.; Li, C.; Shi, G. Q. *J. Am. Chem. Soc.* **2008**, *130*, 5856−5857.
(45) Balapanuru, J.; Yang, J. X.; Xiao, S.; Bao, Q. L.; Jahan, M.; Polavarapu, L.; Wei, J.; Xu, Q. H.; Loh, K. P. *Angew. Chem., Int. Ed.* **2010**, *49*, 6549−6553.
(46) Adhikari, B.; Nanda, J.; Banerjee, A *Chem.—Eur. J.* **2011**, *17*, 11488−11496.
(47) Choi, E. Y.; Han, T. H.; Hong, J.; Kim, J. E.; Lee, S. H.; Kima, H. W.; Kim, S. O. *J. Mater. Chem.* **2010**, *20*, 1907−1912.
(48) An, X.; Simmons, T.; Shah, R.; Lewis, K. M.; Kar, S. *Nano Lett.* **2010**, *10*, 4295−4301.
(49) Zhang, M.; Parajuli, R. R.; He, H. *Small* **2010**, *6*, 1100−1107.
(50) Liang, J. J.; Xu, Y. F.; Sui, D.; Chen, Y. S. *J. Phys. Chem. C* **2010**, *114*, 17465−17471.
(51) Sclafani, J. A.; Maranto, M. T.; Sisk, T. M. *Tetrahedron Lett.* **1996**, *37*, 2193−2196.
(52) aaHummers, W. S.; Offeman, R. E. *J. Am. Chem. Soc.* **1958**, *80*, 1339−1339.
(53) Kovtyukhova, N. I.; Ollivier, P. J.; Martin, B. R.; Mallouk, T. E.; Chizhik, S. A.; Buzaneva, E. V.; Gorchinskiy, A. D. *Chem. Mater.* **1999**, *11*, 771−778.

(54) Li, D.; Muller, B. M.; Gilje, S.; Kaner, R. B.; Wallace, G. G. *Nature Nanotechnology* **2008**, *3*, 101−105.
(55) He, Y.; Su, Y.; Yang, X.; Kang, Z.; Xu, T.; Zhang, R.; Fan, C.; Lee, S. T. *J. Am. Chem. Soc.* **2009**, *131*, 4434−4438.
(56) Hunter, C. A; Sanders, J. M. K. *J. Am. Chem. Soc.* **1990**, *112*, 5525−5534.
(57) Zhao, J.; Lu, J. P.; Han, J.; Yang, C. K. *Appl. Phys. Lett.* **2003**, *82*, 3746−3748.
(58) Balapanuru, J.; Yang, J. X.; Xiao, S.; Bao, Q. L.; Jahan, M.; Polavarapu, L.; Wei, J.; Xu, Q. H.; Loh, K. P. *Angew. Chem., Int. Ed.* **2010**, *49*, 6549−6553.
(59) Ghosh, A.; Rao, K. V.; George, S. J.; Rao, C. N. R. *Chem. Eur. J.* **2010**, *16*, 2700−2704.
(60) Adhikari, B.; Nanda, J.; Banerjee. *Chem. Eur. J.* **2011**, *17*, 11488−11496.
(61) Naughton, K. P. M.; Groves, J. T. *Org. Lett.* **2003**, *5*, 1829−1832.
(62) Bacchi, A.; Biemmi, M.; Carcelli, M.; Carta, F.; Compari, C.; Fisicaro, E.; Rogolino, D.; Sechi, M.; Sippel, M.; Sotriffer, C. A.; Sanchez, T. W.; Neamati, N. *J. Med. Chem.* **2008**, *52*, 7253−7264.
(63) Kovacs, J.; Jentzsch, E.; Mokhir, A. *Inorg. Chem.* **2008**, *47*, 11965−11971.
(64) Liang, J.; Canary, J. W. *Angew. Chem., Int. Ed.* **2010**, *49*, 7710−7713.
(65) Liu, Z.; Robinson, J. T.; Sun, X. M.; Dai, H. J. *J. Am. Chem. Soc.* **2008**, *130*, 10876−10877.
(66) Sun, X. M.; Liu, Z.; Welsher, K.; Robinson, J. T.; Goodwin, A.; Zaric, S.; Dai, H. J. *Nano Res.* **2008**, *1*, 203−212.
(67) Zhang, L. M.; Xia, J. G.; Zhao, Q. H.; Liu, L. W.; Zhang, Z. J. *Small* **2010**, *4*, 537−544.
(68) Wang, Y.; Li, Z. H.; Hu, D. H.; Lin, C. T.; Li, J. H.; Lin, Y. H. *J. Am. Chem. Soc.* **2010**, *132*, 9274−9276.
(69) Peng, C.; Hu, W. B.; Zhou, Y. T.; Fan, C. H.; Huang, Q. *Small* **2010**, *6*, 1686−1692.